Photomedicine and Laser Surgery
Volume 36, Number 6, 2018

Pp. 290–297
DOI: 10.1089/pho.2017.4360

Effect of 810 nm Near-Infrared Laser on Revascularization of Ischemic Flaps in Rats

Jian-Xun Ma, MD,[1,*] Qing-Mo Yang, MD,[2,*] You-Chen Xia, MD,[1,*]
Wei-Guang Zhang, MD,[3] and Fang-Fei Nie, MD[1]

Abstract

Objective: To investigate the effect of 810 nm near-infrared (NIR) laser on the revascularization of ischemic flaps. ***Background:*** It has long been proved that photobiomodulation therapy (PBMT) improves the blood supply of flaps. NIR laser improves the treatment of hypodermis-located lesions and of flap survival, but basic research on the use of 810 nm NIR laser for ischemic flap revascularization is still lacking. ***Materials and methods:*** We prepared two symmetrical long random-pattern flaps on the backs of 60 rats. Each flap was 6 cm long, 1 cm wide, and 1 cm to the middle line. The flaps were divided into an irradiated flap group and an internal control group. The irradiated flaps underwent postoperative 810 nm laser therapy with the energy density of 11.30 J/cm^2 daily. The control flaps were covered by stainless steel to avoid laser irradiation. We observed the viability of the flaps. The flaps underwent Hematoxylin and Eosin (H&E) staining for the observation of histomorphology, immunohistochemical staining of factor VIII for the capillary count, α-smooth muscle actin for the small arterial count, and vascular endothelial growth factor for the integrated optical density (OD) of the positive stained color. ***Results:*** The irradiated flaps showed significantly better flap survival than the control flaps. H&E staining showed that the irradiated flaps had clear tissue structure and little inflammatory cell infiltration. The control flaps demonstrated comparatively worse results. Vascular endothelial growth factor staining showed that the difference in integrated OD between the irradiated flaps and the control flaps was not statistically significant. α-smooth muscle actin and factor VIII staining showed significantly greater numbers of arterioles and capillaries in the irradiated flaps than the control flaps after 4 days of irradiation. ***Conclusions:*** PBMT with 810 nm NIR laser could enhance ischemic flap revascularization and increase flap viability.

Keywords: 810 nm, near-infrared laser, ischemic flap, revascularization

Introduction

Flap transplantation is one of the most fundamental and common techniques in plastic and reconstructive surgery. Skin flaps have a wide range of uses. They can be used to repair traumatic tissue defects, to cover chronic wounds, and to correct deformities. A random flap based on the longitudinal subdermal plexus can be harvested safely if the length:width ratio in the range of 1.5–2:1, and a ratio exceeding this range is at risk of distal flap necrosis.[1] Axial flaps and free flaps too may develop ischemia and even necrosis if the blood flow is decreased.

Photobiomodulation therapy (PBMT), formerly known as low-level laser therapy (LLLT),[2] is a noninvasive, safe application of light in use for the treatment of a variety of pathophysiological conditions, including inflammation, pain, and chronic wounds, with a few side effects.[3] Moreover, as such a treatment can improve the blood flow, it can be used to improve flap viability.[4]

In this study, we treated ischemic flaps with 810 nm near-infrared (NIR) laser,[5] to observe the effect of this treatment on flap revascularization, and attempted to elucidate the mechanism of action.

Materials and Methods

Animals

This study was conducted in accordance with the Guide for the Care and Use of Laboratory Animals and was approved

[1]Department of Plastic Surgery, Peking University Third Hospital, Beijing, China.
[2]Department of Breast Surgery, First Affiliated Hospital of Xiamen University, Xiamen, China.
[3]Department of Anatomy, Basic Medical Science, Peking University Health Science Center, Beijing, China.
*These authors contributed equally to this work.

by the Animal Ethics Committee of the Peking University Health Science Center (ethics approval number: LA2013-83).

Sixty healthy male Sprague-Dawley rats weighing 350–400 g were housed in the Experimental Animal Center of the Peking University Health Science Center. All animals were given rat chow *ad libitum*.

Experiment

Establishment of animal model and laser irradiation. Each rat was anesthetized by intraperitoneal administration of 0.3% sodium pentobarbital at a dose of 0.1 mL/100 g. The surgical site was prepared by shaving the back and disinfecting the skin with conventional iodine alcohol. With the animal lying in the prone position on the operating table, two symmetrical long random-pattern flaps deep to the fascia were raised on the back. Each flap was located 1 cm from the spinous process of vertebrae, 6 cm long and 1 cm wide. The 1-cm-wide pedicle was located at the intersection of a line joining the two iliac spines (Fig. 1). The flaps were then sutured back to the original position with 5–0 silk stitches. Each rat was housed in a single cage postoperatively.

Laser irradiation was performed on the left flap of the rat, and the right flap served as an internal control. When laser irradiation was applied to the animal, a stainless steel plate with an opening area of 2×8 cm was used to prevent irradiation exposure to the other parts of the animal body (Fig. 2).

The SUNDOM-300IB/213 semiconductor gallium–aluminum–arsenide (GaAlAs) laser machine (Beijing SUNDOM Medical Equipment Co., Ltd.) was utilized. The laser wavelength was 810 nm. This machine had three laser probes, which were arrayed in a straight line, and the interval between each other was 3 cm. Each laser beam had divergence of 40° in horizontal direction and 10° in vertical direction, respectively. Therefore, each spot of the laser beam was a rectangle,

FIG. 1. Flap design. The length:width ratio of the flap is 6:1. The two flaps are designed like mirror images by the midline.

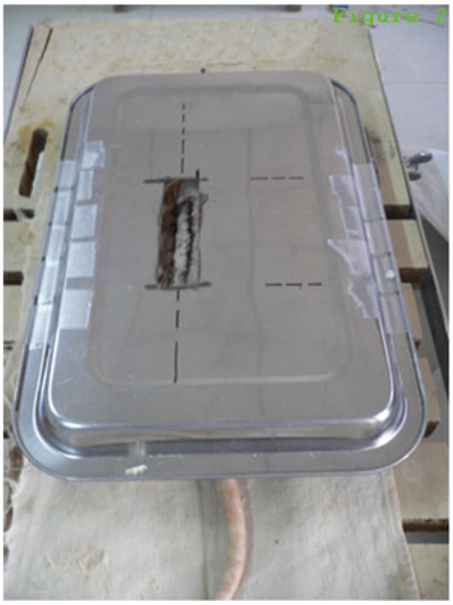

FIG. 2. The internal control side flap (right side) and other parts of the rat are covered by a stainless steel plate when the left side flap is irradiated by the 810 nm NIR laser. NIR, near-infrared.

and the short side was parallel to the line of the three laser probes. The distance between laser probe end point and flap surface was 5 cm. So the spot size of the whole three laser beams was 9.56 cm^2. The output power of each laser beam was set at 100 mW, so the power intensity was 31.38 mW/cm^2. The irradiation time was 6 min, and the energy density was 11.30 J/cm^2.

We fixed the flap on the center of the whole three light spots, and made the long side of the flap parallel to the line of the three laser probes. The light spots could not cover the entire flap. The area of the flap and normal skin in the vicinities, which had been irradiated, was 5.28 cm^2. Total energy delivered to the back of the rat was 59.66 J. Laser irradiation was performed at a laser mode sat on continuous wave, and it was applied once a day under intraperitoneal anesthesia. The rats were divided into four groups on average. Each group was irradiated postoperatively for 4, 7, 10, and 14 days, respectively. The skin flaps were photographed after each irradiation session.

Flap healing and flap survival area

Photographs of the flaps were taken 4–7 days postoperatively when the necrotic areas fixed. Digital images of the skin flaps were analyzed using Image-Pro Plus 6.0 (Media Cybernetics, Inc., Bethesda, MD) to calculate the necrotic areas. Flap survival was calculated using the following formula: flap survival = flap survival area/flap total area $\times$ 100%.

Hematoxylin and eosin and immunohistochemical staining

Four rats chosen from each of four groups were euthanized. The 0.5-cm-long basis and end of both sides of flaps of each rat were collected. These four skin samples underwent routine staining with Hematoxylin and Eosin (H&E). We also

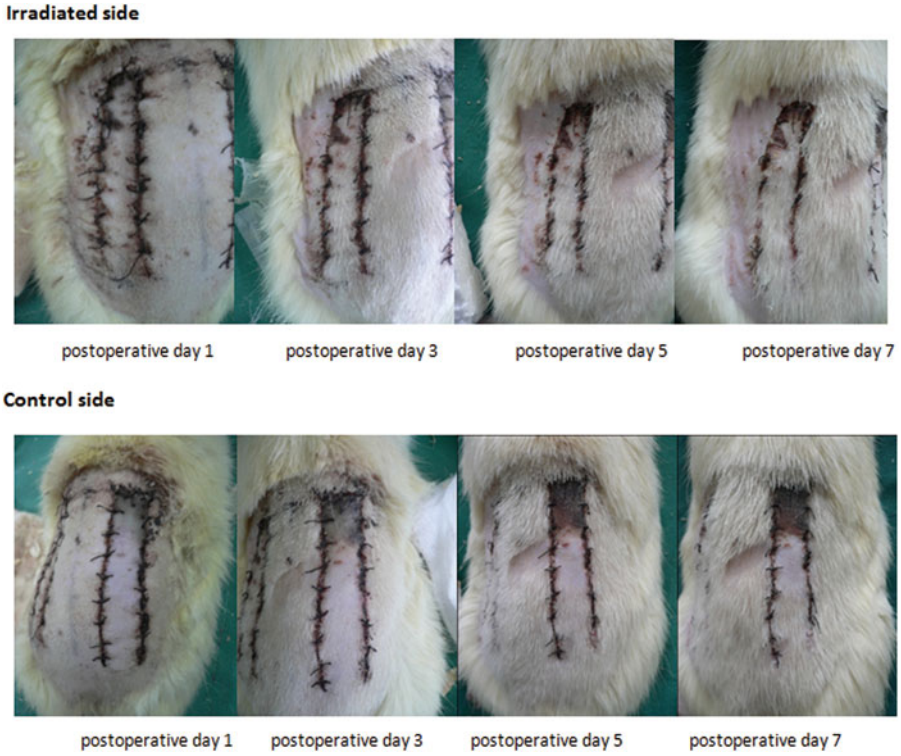

FIG. 3. Flap healing changes on first day, third day, fifth day, and seventh day postoperation, respectively. The irradiated side shows a better flap survival. The control side shows poor healing, early necrosis, and black scab formation.

performed immunohistochemical (IHC) staining of factor VIII for the capillary count, IHC staining of α-smooth muscle actin for the small arterial count, and IHC staining of vascular endothelial growth factor (VEGF) for the integrated optical density (OD) of the positive stained color.

Most of reagents were purchased from Beijjing Zhongshan Golden Bridge Biotechnology Company, Beijing, China. Formalin-fixed, paraffin-embedded tissue sections (4 μm thick) underwent deparaffinization, stepwise rehydration, and endogenous peroxide blockage. For both factor VIII and α-smooth muscle actin staining, slides were processed with antigen retrieval achieved by boiling the slides in citrate buffer (pH 6.0) for 1.5 min. For VEGF staining, slides were boiled in an EDTA solution for 20 min before cooling. Nonspecific binding was blocked using 10% nonimmune goat serum (ZLI-9021) for 10 min. Sections were incubated for 120 min at room temperature with factor VIII antibody (ZA-0111) at a 1:200 dilution, anti-VEGF antibody (ZA-0509) at a 1:100 dilution, or α-smooth muscle actin antibody (ZM-0003) at a 1:100 dilution.

After rinsing, the sections for IHC staining of VEGF and α-smooth muscle actin were incubated with secondary antibodies labeled with HRP (K5007, EnVision™ Detection System, Dako, Denmark) for 30 min at 37°C followed by visualization with diaminobenzidine (DAB+) chromogen (K5007, EnVision™ Detection System), counterstained with Hematoxylin, dehydrated, and mounted. But the sections for VEGF OD analysis were not counterstained with Hematoxylin following visualization with DAB chromogen, which aimed for more accurate analytic results. The sections for ICH staining of factor VIII were incubated with biotinylated secondary antibody (ZB-2010) at a 1:300 dilution for 60 min at 37°C. After rinsing again, these sections were incubated with alkaline phosphatase streptavidin (ZB-2422) at a 1:500 dilution for 60 min at 37°C followed by visualization with BCIP/NBT (ZLI-9041), counterstained with Eosin, dehydrated, and mounted.

Negative controls were processed using the same procedure, except the absence of the primary antibodies. No detectable staining was observed in any of the negative control slides.

In IHC staining of factor VIII, the boundaries of capillaries were stained purple. Ten visual fields (400×) were chosen randomly in each slide of basis of both side flaps for capillary count. Then we calculated the mean count, respectively.

In IHC staining of α-smooth muscle actin, the boundaries of arterioles were stained brown. Ten visual fields (400×) were chosen randomly in each slide of basis of both side flaps for arteriole count. Then we calculated the mean count, respectively.

In IHC staining of VEGF, the positive expression was cytoplasm stained brown. Image-Pro Plus 6.0 was used for quantified analysis to calculate the integrated OD of positive stained color (brown color) of each slide of basis of both slide flaps. Then we calculated the mean OD, respectively.

Statistical analysis

Data were analyzed using SPSS 23.0 and expressed as mean ± standard deviation. Data were analyzed using a standard *t*-test, and significance was denoted by p values <0.05.

Results

Flap survival area

All rats demonstrated a steady increase in necrosis size as time progressed (Fig. 3). At 4–7 days postoperatively when the necrotic areas fixed, the irradiated flaps showed significantly more survival areas (85.99% ± 10.03%) than that of the internal control flaps (81.76% ± 10.62%) ($p < 0.01$).

Histomorphology assessment

H&E staining. In the end of irradiated flaps, the structure of the dermomuscular layer was slightly disordered and there was a large number of subcutaneous inflammatory cell infiltration. While in the end of internal constrol flaps, the dermomuscular layer was atrophied and there was a significant accumulation of inflammatory cells.

In the basis of irradiated flaps, tissue structure was discernible with sufficient subcutaneous vasculature and the muscle fibers of the dermomuscular layer arranged regularly. There was only little inflammatory cell infiltration. As for the basis of internal control flaps, the subcutaneous vasculature and muscle fibers of the dermomuscular layer were still rich without shrinkage, but poorly colored. Muscle cells were swollen and there were more inflammatory cell infiltration (Fig. 4).

Capillary count of factor VIII-related antigen IHC staining

The end of both side flaps demonstrated scabbing, necrosis, and uniform pink eosin staining under microscopy without purple capillaries distribution. The basis of flaps demonstrated rich capillaries, as shown in Fig. 5. The capillary count of basis of both side flaps is shown in Table 1. The results showed that the capillary count of the irradiated flaps was significantly higher than that of the internal control flaps ($p < 0.05$); however, there was no significant difference in the 4-day group.

Small artery count of anti-α-smooth muscle actin IHC staining

The small artery's distribution in the epidermis and subcutaneous connective tissue is shown in Fig. 6. The small artery count of the basis of both side flaps is shown in Table 2. The results showed that the number of small arteries in the irradiated flaps was significantly higher than that in the internal control flaps ($p < 0.05$); however, there was no significant difference in the 4-day group.

OD of VEGF IHC staining

Weak expression of VEGF was present at the end of the flaps. However, high expression of VEGF was present in the basis of the flaps, especially in vascular endothelium and dermomuscular layer (Fig. 7). The OD of the basis of both

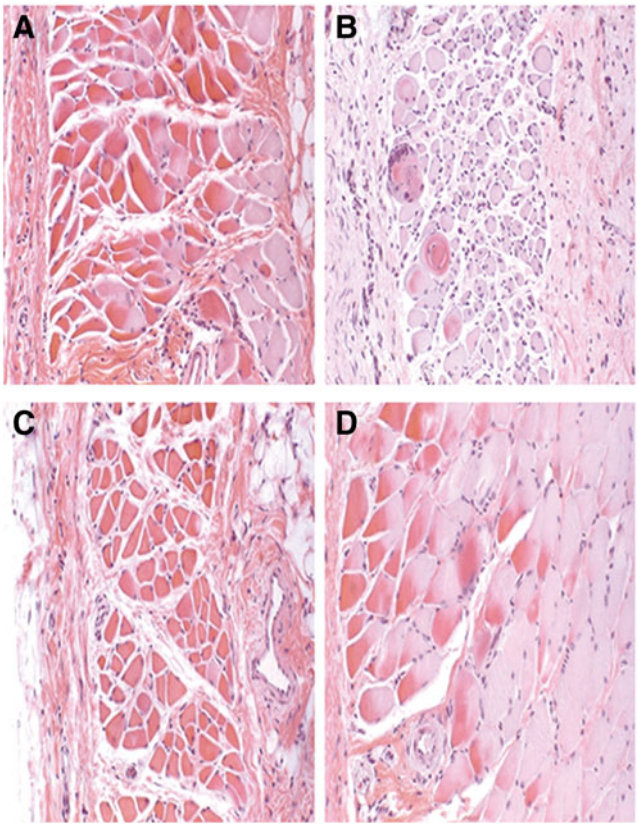

FIG. 4. HE staining (200×) of both side flaps after 14 days of irradiation. **(A)** End of the irradiated flap. The dermomuscular layer has survived, but is slightly disordered and the tissue shows a large number of inflammatory cell infiltration. **(B)** End of the control flap. The dermomuscular layer is atrophied and necrotic with marked infiltration of inflammatory cells. **(C)** Basis of the irradiated flap. The structure of the dermomuscular layer is discernible and arranges regularly. There are few inflammatory cells. **(D)** Basis of the control flap. The dermomuscular layer shows structural disorder and poor stain uptake. The tissue shows a certain number of inflammatory cell infiltration.

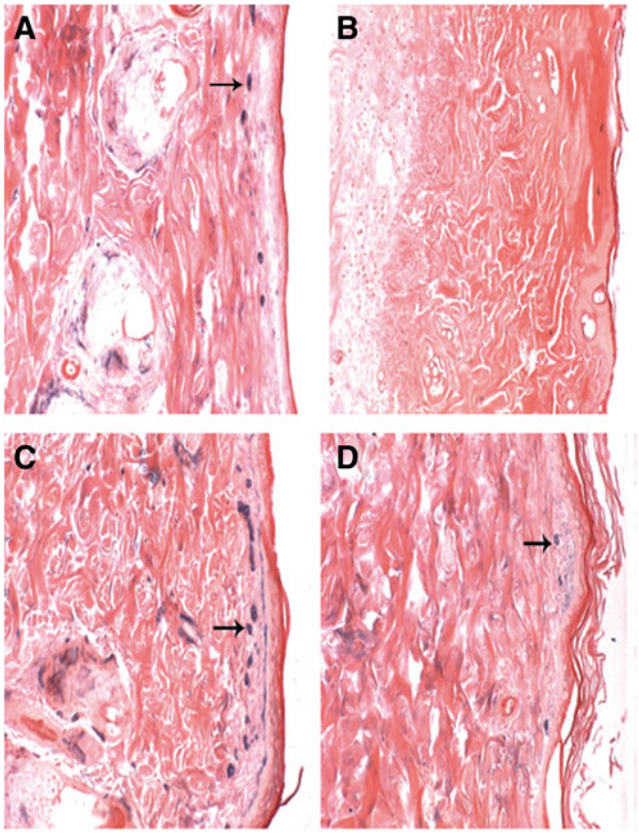

FIG. 5. Factor VIII IHC staining (200×) of both side flaps after 14 days of irradiation, (arrow, capillary). **(A)** End of the irradiated flap. Small number of capillaries. **(B)** End of the control flap. Fewer capillaries. **(C)** Basis of the irradiated flap. More capillaries are distributed under the epidermis. **(D)** Basis of the control flap. Epidermal structural disorder and fewer capillaries. IHC, immunohistochemical.

Table 1. Capillary Count

Grouping (days)	*The irradiated flap*	*The internal control flap*
4	2.44 ± 1.01	2.00 ± 0.71
7	4.25 ± 0.86[a]	2.60 ± 0.84
10	4.94 ± 1.09[a]	2.70 ± 0.95
14	5.72 ± 1.62[a]	3.90 ± 1.52

[a]Compared with the internal control flap, $p < 0.05$.

Table 2. Small Artery Count

Grouping (days)	*The irradiated flap*	*The internal control flap*
4	4.67 ± 0.82	3.78 ± 1.09
7	8.37 ± 1.89[a]	6.67 ± 1.94
10	8.40 ± 2.67[a]	5.90 ± 1.51
14	10.55 ± 2.02[a]	8.10 ± 2.38

[a]Compared with the internal control flap, $p < 0.05$.

side flaps is shown in Table 3. The OD of the irradiated flaps was slightly higher than that of the internal control flaps, but without statistical significance ($p > 0.05$).

Discussion

LLLT, which has been applied for more than 40 years,[6] is now denominated as PBMT.[2] The PBMT can result in beneficial therapeutic outcomes, including but not limited to the alleviation of pain or inflammation, promotion of wound healing, and tissue regeneration.[2] All of these effects are not mediated through the thermal increase, which is one of the most distinguishing features of PBMT as compared with other photoceutical modalities.[7] The basic biological mechanism of the effects of PBMT is thought to be through absorption of low-level laser by chromophores, in particular cytochrome c oxidase (CCO), which is complex IV of the mitochondrial respiratory chain.[8] Then the cells activate retrograde light-sensitive cellular signaling events to transport the light signal from mitochondria to nucleus, which eventually alter the cellular metabolism and functions.[9] The mitochondrial photoacceptor, CCO, is identified as a principal tissue chromophore for visible/NIR spectral light.[8]

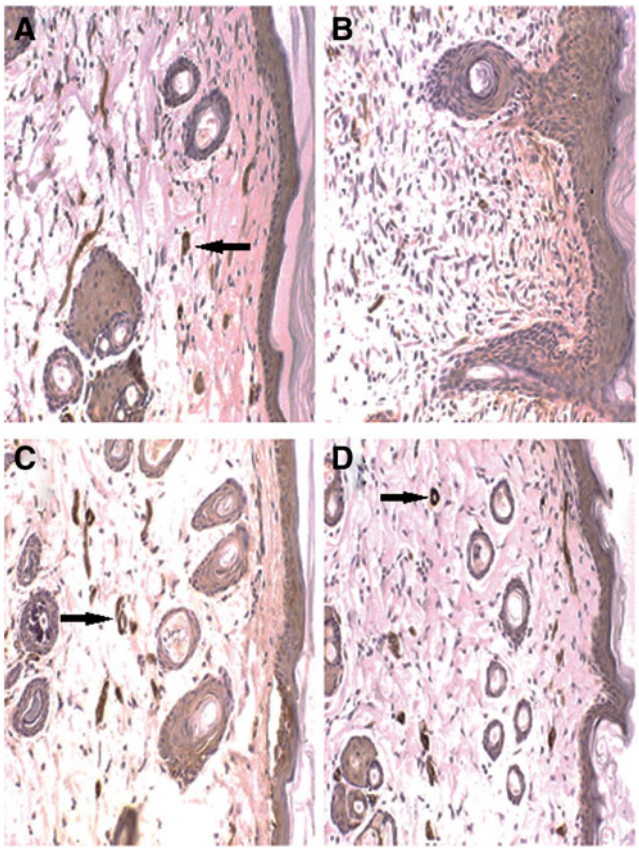

FIG. 6. α-smooth muscle actin IHC staining (200×) of both side flaps after 14 days of irradiation, (arrow, arteriole). **(A)** End of the irradiated flap. A few arterioles under the epidermis. **(B)** End of the control flap. No arterioles. **(C)** Basis of the irradiated flap. More arterioles under the epidermis. **(D)** Basis of the control flap. Epidermal structural disorder and fewer arterioles.

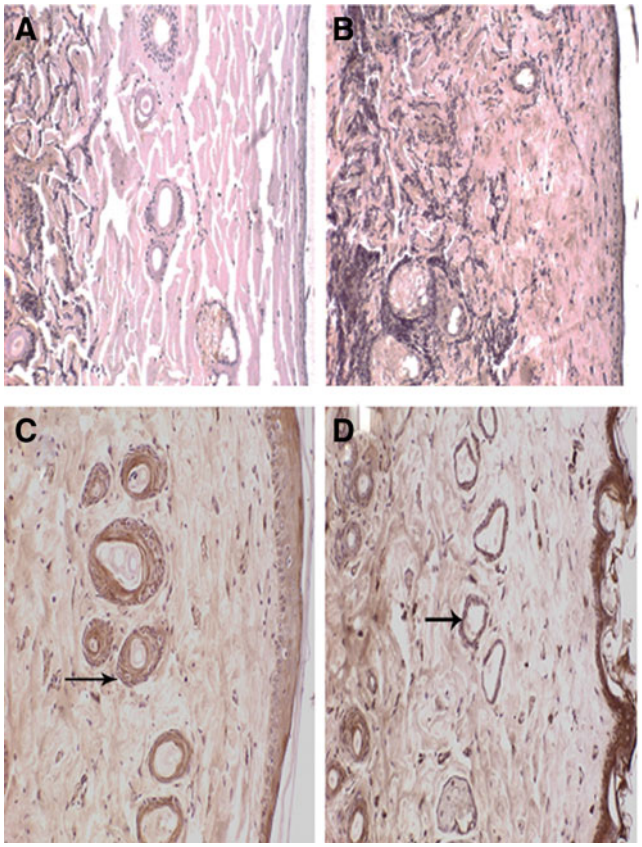

FIG. 7. VEGF IHC staining (200×) of both side flaps after 14 days of irradiation, (arrow, expression of VEGF). **(A)** End of the irradiated flap. Few blood vessels and weak VEGF expression under the epidermis. **(B)** End of the control flap. Epidermal structure disorder and inflammatory cell distribution. No VEGF expression. **(C)** Basis of the irradiated flap. Many blood vessels under the skin, strong VEGF expression on blood vessels. **(D)** Basis of the control flap. Many blood vessels under the skin, strong VEGF expression on blood vessels. VEGF, vascular endothelial growth factor.

Table 3. Vascular Endothelial Growth Factor Optical Density Value

Grouping (days)	*The irradiated flap*	*The internal control flap*
4	0.1090 ± 0.0217[a]	0.0830 ± 0.0416
7	0.1137 ± 0.0278[a]	0.0913 ± 0.0448
10	0.0914 ± 0.0530[a]	0.1090 ± 0.0350
14	0.1070 ± 0.0650[a]	0.0750 ± 0.0280

[a]Compared with the internal control flap, $p > 0.05$.

The tissue–light interaction primarily depends on wavelength, as it determines the absorption mechanism and the depth of penetration.[10] PBMT generally employs light at red (630–680 nm) and NIR (800–830 nm) wavelengths to modulate biological activities,[11] as they are highly active in the healing process.[12–14]

Red light is readily absorbed by blood and skin surface components, thereby limiting its tissue penetration to <10 mm. While NIR light is not readily absorbed and has a much deeper depth of tissue penetration (30–40 mm or more), this provides a greater deposition of photons into the wound bed, and show therapeutic healing efficacy.[15] Moreover, biological tissue has lower scattering capacity at the NIR region than at the visible region,[16] because CCO has distinct absorption bands in the red and in the NIR regions.[13] So NIR is found to be the most effective and widely studied wavelength range followed by red light exhibiting beneficial photobiomodulatory effects on impaired dermal wound healing, which could be attributed to the greater penetration and to the absorption spectrum of CCO.[15,16] To investigate the revascularization of ischemic flaps, target tissues applied with PBMT are located deeper under the skin. From this perspective, 810 nm NIR laser was selected in our study.

Flap survival area

In our study, improvement of ischemic flap survival was the most apparent performance of the 810 nm NIR laser irradiation. Flap revascularization could be observed by the naked eye.

According to Bossini's experiment,[17] 670 nm laser effectively increased the viability of the skin flap and energy density of 24 J/cm^2 was more effective than 12, 6, and 3 J/cm^2, so there was a tendency for better results at higher energy density. While other studies demonstrated that too high energy density of light had deleterious effects on cells by inducing apoptosis through generation of high levels of reactive oxygen species.[18,19] Previous research indicated that the effect of wound repair improvement by PBMT was a result of an inversely proportional relationship between wavelength and fluence, with treatment more effective when combining higher fluence with shorter wavelength or lower fluence with longer wavelength.[20]

Al-Watban[21] demonstrated wound healing of diabetic rats was markedly accelerated after PBMT at 810 nm by fluence of 5 and 10 J/cm^2 (not at 20 and 30 J/cm^2). Similarly, PBMT at 808 nm (GaAlAs) and 10 J/cm^2 could improve incisional wound healing.[22] In our study, to improve ischemic flap survival, 810 nm laser irradiation was performed daily in our study with energy density of 11.30 J/cm^2 and total energy of 59.66 J. The present experimental results did show that 810 nm NIR lasers reduced the necrotic area as evidenced by the survival area of up to $85.99\% \pm 10.03\%$. Whether the fluence used in the present study was optimal still needed further research. However, these data indicated a positive effect of 810 nm NIR laser therapy on flap survival.

The result of better survival revealed that the 810 nm NIR laser irradiation might strongly promote revascularization, accelerate healing, and then reduce necrosis. The effect of revascularization promotion and healing acceleration had been proven by many studies. Kubota[23] showed increased blood flow and perfusion of transferred flaps after irradiation with an 830 nm NIR laser. Gupta[15] and Keshri[24] both demonstrated healing efficacy of 810 nm NIR laser PBMT on dermal wounds. Our finding of the necrosis reduction by 810 laser irradiation was in agreement with other studies. Prado,[25] for instance, indicated 830 nm laser was effective in increasing skin flap viability in rats. In addition, das Neves[26] found that PBMT with 830 nm laser decreased the area of necrosis in rats subjected to nicotine, which had been confirmed to have the deleterious effect on skin flap.

Morphological changes

Naked eye results are supported by the histological patterns, which can offer some information about the mechanism responsible for the improved flap survival. Surgical trauma to the body causes inflammatory reactions. Intense inflammatory response may cause flap edema and pain. Moreover, tissue swelling may decrease blood flow velocity and reduce the nutrient supply of the flap. However, PBMT can be used for anti-inflammatory treatment, which has been confirmed by previous studies.[27,28] In addition, there were some other researches that had the same results. Pinfildi[29] indicated that PBMT could stimulate mast cell growth in flaps to increase vascular perfusion. Albertini[30] found that red laser (660 and 684 nm) PBMT significantly reduced carrageenan-induced paw edema, and muscle inflammation was also significantly reduced in rats. All of these showed that PBMT could reduce inflammation and edema and inhibit inflammatory cell migration.

As for NIR laser, positive effect on the reduction of inflammatory cell infiltration was still significant. Keshri[24] demonstrated that 810 nm PBMT could reduce inflammatory infiltration and enhance fibroblast proliferation, angiogenesis, and re-epithelialization in the wound tissues of immunosuppressed rats. The study of Rezende[31] suggested that 830 nm NIR laser irradiation could act on the cellular events that happen during inflammatory stage, and the reduction on the duration of the inflammatory stage might result in a faster entry into the proliferative stage of healing. Moreover, their histological analysis also showed a lower polymorphonuclear infiltration in irradiated lesions than control lesions. Study of Pallotta[32] also indicated that 810 nm PBMT was able to significantly inhibit the total number of leukocytes, which was confirmed by cell counting showing the reduction of polymorphonuclear cells at the inflammatory site.

In our study, HE staining showed that the inflammatory cells in the irradiated flaps were significantly less than that in the internal control flaps, which demonstrated that the flaps treated with 810 nm NIR laser irradiation healed well, whereas the flaps that were not irradiated became swollen due to inflammatory exudation and healed slowly. Therefore, reduction on the duration of the inflammatory stage might promote

revascularization of ischemic flaps, sequentially improve the healing, and reduce the area of necrosis.

The revascularization rate directly affects the survival of flap transplanted. VEGF can promote the growth of vascular endothelial cells and the formation of blood vessels. PBMT had been demonstrated to increase the gene expression and release of VEGF by cells.[33] Prado[34] found that 830 nm PBMT promoted flap expression of VEGF and angiogenesis, and sequentially reduced flap necrosis. Keshri[24] also demonstrated VEGF expression increased significantly in the 810 nm laser irradiation group than the control group. Our study showed that 810 nm laser irradiation promoted VEGF synthesis in, and secretion from, the basis of the flaps. But the expression of VEGF between the irradiated side and the internal control side was not significantly different, which was not consistent with previous studies. We thought it possible that VEGF of irradiated flap went to adjacent cells or tissue of the internal control flap, which was on the same rat, through paracrine mode.[35] But we did not test it in this study.

VEGF can also promote vascular proliferation within flaps. Yaakobi[36] used 804 nm laser to treat rats with myocardial infarction by ligation of the left anterior descending artery. They found the myocardial infarction size was reduced significantly after the irradiation, and neovascularization rate of the laser irradiation group was 3.1 times higher than that of the control group, which was a significant increase. Oron[37] demonstrated 810 nm PBMT applied to mdx mice during postnatal development might have a significant beneficial effect in the process of skeletal muscle regeneration and angiogenesis.

Our study also found significant changes of vascular proliferation in the flaps on the irradiated side. The factor VIII-related antigen IHC staining for capillaries and anti-α-smooth muscle actin IHC staining for small arteries showed higher number of blood vessels in the irradiated flaps than the internal control flaps. This phenomenon became apparent with continuous irradiation more than 4 days, and there was an increasing trend. The previous study[26] also demonstrated that 830 nm NIR laser could increase the number of blood vessels of flaps, and consequently, decrease the area of necrosis. In addition, the proliferation of blood vessels of the 4-day group in our study showed no statistically significant difference between the irradiated side and the internal control side, indicating that the effect of 810 nm laser on angiogenesis became prominent after 4 days of irradiation. These data suggested that it took a few days for endothelial cells to form vascular structures.

Our data suggested that the increased number of blood vessels was closely related to the 810 nm laser irradiation, which resulted in more perfusion of blood in the ischemic flaps and in the decrease of the necrotic area of the end of ischemic flaps.

Conclusions

The focus of this research was the 810 nm NIR laser effect on the revascularization of ischemic flaps on the rats. Our findings indicated that PBMT with 810 nm laser, at the tested parameters, inhibited excessive inflammation and facilitated angiogenesis, so improving revascularization, promoting flap healing, and enhancing skin flap survival. Nevertheless, further studies should be conducted to find optimal therapeutic parameters and to determine the efficacy of 810 nm NIR laser irradiation on patients for clinical application.

Acknowledgments

The authors thank Jian-Ning Li, Yong-Guang Ma, Dong Li, and Li Chen for assisting with the experiment.

Author Disclosure Statement

This work was supported by the Scientific Seed Fund of Peking University Third Hospital.

References

1. Scott L. Hansen, David M. Young, Patrick Lang, Hani Sbitany. Flap classification and applications. In: Plastic Surgery Volumes One: Principles, 3rd ed. Gurtner GC (ed.). London: Elsevier Saunders, 2013, p. 512.
2. Anders JJ, Lanzafame RJ, Arany PR. Low-level light/laser therapy versus photobiomodulation therapy. Photomed Laser Surg 2015;33:183–184.
3. Herranz-Aparicio J, Vázquez-Delgado E, Arnabat-Domínguez J, España-Tost A, Gay-Escoda C. The use of low level laser therapy in the treatment of temporomandibular joint disorders. Review of the literature. Med Oral Patol Oral Cir Bucal 2013;18:e603–e612.
4. Hersant B, SidAhmed-Mezi M, Bosc R, Meninqaud JP. Current indications of low-level laser therapy in plastic surgery: a review. Photomed Laser Surg 2015;33:283–297.
5. De Freitas LF, Hamblin MR. Proposed mechanisms of photobiomodulation or low-level light therapy. IEEE J Sel Top Quantum Electron 2016;22:pii:7000417.
6. Mester E, Korényi-Both A, Spiry T, Tisza S. The effect of laser irradiation on the regeneration of muscle fibers (preliminary report). Z Exp Chir 1975;8:258–262.
7. Lin F, Josephs SF, Alexandrescu DT, et al. Lasers, stem cells, and COPD. J Transl Med 2010;8:16.
8. Karu Tl, Kolyakov SF. Exact action spectra for cellular responses relevant to phototherapy. Photomed Laser Surg 2005;23:355–361.
9. Passarella S, Karu T. Absorption of monochromatic and narrow band radiation in the visible and near IR by both mitochondrial and non-mitochondrial photoacceptors results in photobiomodulation. J Photochem Photobiol B 2014;140:344–358.
10. Capon A, Mordon S. Can thermal lasers promote skin wound healing? Am J Clin Dermatol 2003;4:1–12.
11. Chung H, Dai T, Sharma SK, Huang YY, Carroll JD, Hamblin MR. The nuts and bolts of low-level laser (light) therapy. Ann Biomed Eng 2012;40:516–533.
12. Wu Q, Xuan W, Ando T, et al. Low-level laser therapy for closed-head traumatic brain injury in mice: effect of different wavelengths. Lasers Surg Med 2012;44:218–226.
13. Karu TI, Pyatibrat LV, Kolyakov SF, Afanasyeva NI. Absorption measurements of a cell monolayer relevant to phototherapy: reduction of cytochrome c oxidase under near IR radiation. J Photochem Photobiol B 2005;81:98–106.
14. Thunshelle C, Hamblin MR. Transcranial low-level laser (light) therapy for brain injury. Photomed Laser Surg 2016;34:587–598.
15. Gupta A, Dai T, Hamblin MR. Effect of red and near-infrared wavelengths on low-level laser (light) therapy-induced

healing of partial-thickness dermal abrasion in mice. Lasers Med Sci 2014;29:257–265.
16. Yadav A, Gupta A. Noninvasive red and near-infrared wavelength-induced photobiomodulation: promoting impaired cutaneous wound healing. Photodermatol Photoimmunol Photomed 2017;33:4–13.
17. Bossini PS, Fangel R, Habenschus RM, et al. Low-level laser therapy (670 nm) on viability of random skin flap in rats. Lasers Med Sci 2009;24:209–213.
18. Wu S, Xing D, Gao X, Chen WR. High fluence low-power laser irradiation induces mitochondrial permeability transition mediated by reactive oxygen species. J Cell Physiol 2009;218:603–611.
19. Huang L, Wu S, Xing D. High fluence low-power laser irradiation induces apoptosis via inactivation of Akt/GSK3β signaling pathway. J Cell Physiol 2011;226:588–601.
20. Do Nascimento PM, Pinheiro AL, Salgado MA, Ramalho LM. A preliminary report on the effect of laser therapy on the healing of cutaneous surgical wounds as a consequence of an inversely proportional relationship between wavelength and intensity: histological study in rats. Photomed Laser Surg 2004;22:513–518.
21. Al-Watban FA, Zhang XY, Andres BL. Low-level laser therapy enhances wound healing in diabetic rats: a comparison of different lasers. Photomed Laser Surg 2007;25:72–77.
22. Güngörmüs M, Akyol UK. Effect of biostimulation on wound healing in diabetic rats. Photomed Laser Surg 2009;27:607–610.
23. Kubota J. Effects of diode laser therapy on blood flow in axial pattern flaps in the rat model. Lasers Med Sci 2002;17:146–153.
24. Keshri GK, Gupta A, Yadav A, Sharma SK, Singh SB. Photobiomodulation with pulsed and continuous wave near-infrared laser (810 nm, Al-Ga-As) augments dermal wound healing in immunosuppressed rats. PLoS One 2016;11:e0166705.
25. Prado RP, Pinfildi CE, Liebano RE, Hochman BS, Ferreira LM. Effect of application site of low-level laser therapy in random cutaneous flap viability in rats. Photomed Laser Surg 2009;27:411–416.
26. das Neves LM, Marcolino AM, Prado RP, Ribeiro Tde S, Pinfildi CE, Thomazini JA. Low-level laser therapy on the viability of skin flap in rats subjected to deleterious effect of nicotine. Photomed Laser Surg 2011;29:581–587.
27. Parirokh M, Dabiri S, Bahrampour A, Homayon Zadeh M, Eghbal MJ. Effect of low power laser on incisional wound healing. Iran Endod J 2006;1:157–160.
28. Rabelo SB, Villaverde AB, Nicolau R, Salgado MC, Melo Mda S, Pacheco MT. Comparison between wound healing in induced diabetic and nondiabetic rats after low-level laser therapy. Photomed Laser Surg 2006;24:474–479.
29. Pinfildi CE, Liebano RE, Hochman BS, et al. Effect of low-level laser therapy on mast cells in viability of the transverse rectus abdominis musculocutaneous flap. Photomed Laser Surg 2009;27:337–343.
30. Albertini R, Villaverde AB, Aimbire F, et al. Anti-inflammatory effects of low-level laser therapy (LLLT) with two different red wavelengths (660 nm and 684 nm) in carrageenan-induced rat paw edema. J Photochem Photobiol B 2007;89:50–55.
31. Rezende SB, Ribeiro MS, Núñez SC, Garcia VG, Maldonado EP. Effect of a single near-infrared laser treatment on cutaneous wound healing: biometrical and histological study in rats. J Photochem Photobiol B 2007;87:145–153.
32. Pallotta RC, Bjordal JM, Frigo L, et al. Infrared (810-nm) low-level laser therapy on rat experimental knee inflammation. Lasers Med Sci 2012;27:71–78.
33. Peplow PV, Baxter GD. Gene expression and release of growth factors during delayed wound healing: a review of studies in diabetic animals and possible combined laser phototherapy and growth factor treatment to enhance healing. Photomed Laser Surg 2012;30:617–636.
34. Prado RP, Garcia SB, Thomazini JA, Piccinato CE. Effects of 830 and 670 nm laser on viability of random skin flap in rats. Photomed Laser Surg 2012;30:418–424.
35. Schlosser S, Dennler C, Schweizer R, et al. Paracrine effects of mesenchymal stem cells enhance vascular regeneration in ischemic murine skin. Microvasc Res 2012;83:267–275.
36. Yaakobi T, Shoshany Y, Levkovitz S, Rubin O, Ben Haim SA, Oron U. Long-term effect of low energy laser irradiation on infarction and reperfusion injury in the rat heart. J Appl Physiol (1985) 2011;90:2411–2419.
37. Oron A, Oron U, Sadeh M. Low-level laser therapy during postnatal development modulates degeneration and enhances regeneration processes in the hindlimb muscles of dystrophic mice. Photomed Laser Surg 2014;32:606–611.

Address correspondence to:
You-Chen Xia
Department of Plastic Surgery
Peking University Third Hospital
#49, North Garden Road
Haidian District
Beijing 100191
P.R. China

E-mail: xiayouch@126.com

Received: July 17, 2017.
Accepted after revision: March 8, 2018.
Published online: June 5, 2018.